HHS Public Access

Author manuscript

Neuroimage. Author manuscript; available in PMC 2019 July 01.

Published in final edited form as:

Neuroimage. 2019 March ; 188: 572–583. doi:10.1016/j.neuroimage.2018.12.009.

Vascular burden and APOE ε4 are associated with white matter microstructural decline in cognitively normal older adults

Owen A. Williams[a], **Yang An**[a], **Lori Beason-Held**[a], **Yuankai Huo**[b], **Luigi Ferrucci**[c], **Bennett A. Landman**[b], and **Susan M. Resnick**[a,*]

[a]Laboratory of Behavioral Neuroscience, National Institute on Aging, Baltimore, MD 21224, USA

[b]School of Engineering, Vanderbilt University, Nashville, TN 37212, USA

[c]Longitudinal Studies Section, Translational Gerontology Branch, National Institute on Aging, Baltimore, MD 21224, USA

Abstract

White matter microstructure can be measured with diffusion tensor imaging (DTI). While increasing age is a predictor of white matter (WM) microstructure changes, roles of other possible modifiers, such as cardiovascular risk factors, APOE ε4 allele status and biological sex have not been clarified.

We investigated 665 cognitively normal participants from the Baltimore Longitudinal Study of Aging (age 50–95, 56.7% female) with a total of 1384 DTI scans. WM microstructure was assessed by fractional anisotropy (FA) and mean diffusivity (MD). A vascular burden score was defined as the sum of five risk factors (hypertension, obesity, elevated cholesterol, diabetes and smoking status). Linear mixed effects models assessed the association of baseline vascular burden on baseline and on rates of change of FA and MD over a mean follow-up of 3.6 years, while controlling for age, race, and scanner type. We also compared DTI trajectories in *APOE* ε4 carriers vs. noncarriers and men vs. women.

At baseline, higher vascular burden was associated with lower FA and higher MD in many WM structures including association, commissural, and projection fibers. Higher baseline vascular burden was also associated with greater longitudinal decline in FA in the hippocampal part of the cingulum and the fornix (crus)/stria terminalis and splenium of the corpus callosum, and with greater increases in MD in the splenium of the corpus callosum. *APOE* ε4 carriers did not differ from non-carriers in baseline DTI metrics but had greater decline in FA in the genu and splenium of the corpus callosum. Men had higher FA and lower MD in multiple WM regions at baseline but showed greater increase in MD in the genu of the corpus callosum. Women showed greater decreases over time in FA in the gyrus part of the cingulum, compared to men.

Our findings show that modifiable vascular risk factors (1) have a negative impact on white matter micro-structure and (2) are associated with faster microstructural deterioration of temporal WM regions and the splenium of the corpus callosum in cognitively normal adults. Reducing vascular

*Corresponding author. owen.williams@nih.gov (O.A. Williams), resnicks@mail.nih.gov (S.M. Resnick).

Appendix A. Supplementary data

Supplementary data to this article can be found online at https://doi.org/10.1016/j.neuroimage.2018.12.009.

burden in aging could modify the rate of WM deterioration and could decrease age-related cognitive decline and impairment.

Keywords

Diffusion tensor imaging (DTI) White matter microstructure Aging Vascular risk factors Apolipoprotein ε4

1. Introduction

Altered white matter microstructure has been associated with age-related cognitive decline and dementia (Bendlin et al., 2010; Charlton et al., 2010; Di Paola, Spalletta and Caltagirone, 2010; Kennedy and Raz, 2009a,b; Mielke et al., 2012; Nir et al., 2013). A vascular etiology has been proposed and the prevalence of vascular diseases increases with age (Lakatta and Levy, 2003; Thom et al., 2006). Therefore, understanding the relationships between cardiovascular risk factors and white matter degeneration in cognitively normal older adults is important, as it may highlight possible targeted interventions designed to reduce vascular burden and slow/prevent white matter damage before there are cognitive consequences.

Microstructural properties of cerebral white matter can be assessed using diffusion tensor imaging (DTI), a magnetic resonance imaging technique (Basser et al., 1994). Two commonly used DTI metrics are fractional anisotropy (FA) and mean diffusivity (MD). FA is used to quantify the directionality and MD is used to quantify the magnitude of water diffusion within brain tissue. In the white matter, axons, myelin sheaths and neurofilaments restrict both direction and magnitude of diffusion, leading to highly directional diffusion running in parallel with the white matter structures. This leads to high levels of FA in the white matter compared to cerebral grey matter (Pierpaoli et al., 1996). Age-related decreases in FA and increases in MD have been widely reported from both cross-sectional and longitudinal studies and are thought to reflect age-related microstructural damage (Barrick et al., 2010; Charlton et al., 2006; Kennedy and Raz, 2009a,b; Salat et al., 2005; Sexton et al., 2014).

A review of DTI studies in vascular disease concluded that DTI metrics are sensitive to vascular disease related changes, can serve as surrogate markers of white matter microstructure and be used to monitor disease progression (Alves et al., 2012). Various cardiovascular risk factors including hypertension, obesity, elevated total cholesterol, diabetes and cigarette smoking have all been shown to negatively impact white matter regions including association, projection, commissural and limbic fibers (Hoogenboom et al., 2014; Hsu et al., 2012; Karlsson et al., 2013; Mail-lard et al., 2012; McEvoy et al., 2015; Papageorgiou et al., 2017; Reijmer et al., 2013). However, these studies are often limited by small sample sizes, are typically cross-sectional designs and often consider only a single vascular risk factor.

While cross-sectional investigations have revealed promising insights into the relationships between white matter microstructure and cardio-vascular risk factors, they are limited to

providing between-person comparisons. To directly estimate the effect of vascular burden on within-person change in brain structure, longitudinal studies are required. However, there are few longitudinal studies that have assessed the impact of vascular risk factors on trajectories of white matter microstructure in cognitively normal adults. de Groot et al. (2015) found that cardiovascular risk factors were largely unrelated to longitudinal changes in white matter microstructure except for higher total cholesterol which was associated with faster increases in MD over a two-year follow-up. Bender and Raz (2015) found that the effects of cardiovascular risk were limited to faster decline in FA over a two-year period in the body of the corpus callosum and the dorsal cingulum bundle. Longer follow-up time on larger data sets may improve the statistical power to assess the impact of vascular risk factors on white matter microstructural changes.

Investigating the impact of cardiovascular risk factors is complicated by the fact that many risk factors co-exist, e.g. associations between type 2 diabetes and obesity. This makes it difficult for studies to evaluate the individual contribution of an isolated risk factor, but it also makes it necessary to explore additive and cumulative effects of risk factors. Cumulative vascular risk factor scores have previously been shown to be related to increased risk of dementia (Luchsinger et al., 2005) and amyloid pathology (Gottesman et al., 2017) and may prove to be useful tools in evaluating the cumulative impact of vascular risk factors on white matter microstructure.

Two additional, non-modifiable factors that may affect age-related changes in white matter microstructure are Apolipoprotein E (APOE) genotype, i.e., *APOE* ε4 allele status, and sex. Cross-sectional results assessing the impact of the APOE ε4 allele on FA and MD are inconclusive, with Patel et al. (2013) reporting no differences in FA in carriers versus non-carriers, while (Honea et al., 2009) found evidence of reduced FA in the left parahippocampal gyrus in carriers compared to non-carriers. In longitudinal analysis, de Groot et al. (2015) found counterintuitive decreases in MD in carriers compared to non-carriers, while Teipel et al. (2010) found no significant differences between carriers and non-carriers.

Sex differences in DTI measures are not well understood. In several cross-sectional studies, no sex differences in DTI in global white matter or regions of interest (ROIs) were reported (Inano et al., 2011; Kennedy and Raz, 2009; Kennedy and Raz, 2009a,b; Lee et al., 2009; Ota et al., 2006). However, other studies have reported significant sex differences, with men having higher FA in the corpus callosum, thalamus, cingulum and frontal white matter (Menzler et al., 2011; Oh et al., 2007; Szeszko et al., 2003). Longitudinal studies of sex differences in DTI trajectories are limited; however, Sexton et al. (2014) found no sex differences in the rate of decline in FA.

The primary aims of the current study were to investigate associations of the accumulation of cardiovascular risk factors, individual cardiovascular risk factors, and *APOE* ε4 carrier status with white matter macro-structural change in cognitively normal adults in the Baltimore Longitudinal Study of Aging (BLSA). We examine both cross-sectional and longitudinal associations of baseline vascular burden, cardiovascular risk factors, and APOE ε4 status with white matter microstructure and also report effects of age and sex. Given few

longitudinal DTI studies in cognitively normal aging adults, we present this work as an exploratory analysis to investigate regionally specific associations. While DTI metrics vary across regions, they are highly correlated within individuals. Therefore, results were not corrected for multiple comparisons across ROIs.

2. Methods

2.1. Participants

This study uses data from participants in the Baltimore Longitudinal Study of Aging (BLSA), a long running study of physical and psychological aging in community-dwelling adults (Shock, 1984). Participants were included in the current analyses if they were over the age of 50, had undergone a DTI scan between 2009 and 2016 and had concurrent neuropsychological data. 665 participants had DTI data; of these, 406 participants had longitudinal data (two or more DTI scans). Exclusion criteria included diagnoses of mild cognitive impairment (MCI), Alzheimer's disease (AD), dementia, Parkinson's disease or a history of stroke. The participants were also free of significant health conditions that could affect brain structure (i.e. closed head injury, brain surgery, malignant cancer, meningiomas and cysts with brain tissue displacement, seizure and bipolar disorders). Participants were excluded if they had these conditions at baseline or, if they developed these conditions during the follow-up interval; any visits after the onset of a condition were removed. MCI status was determined using the Petersen criteria (Petersen, 2004) for MCI, dementia and AD, respectively, were determined using the Diagnostic and Statistical Manual, third edition, revised (DSM-III-R) (American Psychiatric Association, 1987) and the National Institute of Neurological and Communication Disorders and Stroke-Alzheimer's Disease and Related Disorders Association criteria (McKhann et al., 1984). The mean Mini Mental State Examination score at baseline was 28.6 (standard deviation = 1.4). Parkinson's disease and history of stroke were determined based on self-reported diagnoses. The Institutional Review Board approved the study protocol, and all participants provided informed consent at each visit.

2.2. Vascular burden, vascular risk factors, and APOE ε4 status

A cumulative vascular burden score and its components were assessed. Using a similar approach to Gottesman et al. (2017), the cumulative vascular burden score was a summed score of the total number of cardiovascular risk factors present for each participant. Cardiovascular risk factors included hypertension (systolic blood pressure ≥140 mm Hg and/or diastolic blood pressure ≥90 mm Hg or treatment with antihypertensive medications), obesity (body mass index ≥ 30), elevated total cholesterol (≥200 mg/dl), diabetes (HbA1C ≥ 6.5 or self-report of taking medication to treat diabetes), and smoking status (ever vs never). In statistical analysis, the vascular burden score was treated as a continuous variable. As there were few participants with 4 or 5 cardiovascular risk factors, the score was capped at 3 or more risk factors to ensure a normal distribution.

APOE ε4 status, defined as having at least one ε4 allele, was also evaluated as a binary score comparing carriers vs. non-carriers.

2.3. MRI acquisition

MRI data were acquired on three different 3 T Philips Achieva scanners (scanners 1 and 2 at the Kennedy Krieger Institute and scanner 3 at the National Institute on Aging). DTI acquisition protocol was identical for scanners 1 and 2 but was different for scanner 3:

DTI acquisition, Scanners 1 and 2: number of gradients = 32, number of b0 images = 1, max b-factor = 700 s/mm^2, TR/TE = 6801/75 msec, number of slices = 65, voxel size = 0.83 × 0.83 × 2.2 mm, reconstruction matrix = 256 × 256, acquisition matrix = 96 × 95, field of view = 212 × 212 mm, flip angle = 90°. DTI acquisition, Scanner 3: number of gradients = 32, number of b0 images = 1, max b-factor = 700 s/mm^2, TR/TE = 7454/75 msec, number of slices = 70, voxel size = 0.81 × 0.81 × 2.2 mm, reconstruction matrix = 320 × 320, acquisition matrix = 116 × 115, field of view = 260 × 260mm, flip angle = 90°. Two separate DTI scans were acquired for each participant and subsequently combined to generate images with a number of signal averages = 2 to improve the signal to noise ratio (Lauzon et al., 2013).

2.4. Image analysis

Tensor fitting and quality assessment was carried out using a protocol described previously (Lauzon et al., 2013; Tian et al., 2016). Briefly, diffusion-weighted volumes were affine co-registered to b0 image target to correct for eddy current and physiological motion effects. The gradient tables were corrected for the identified rotational component using finite strain (Alexander et al., 2001). To combine the two DTI sessions that had different unknown intensity normalization constants, each diffusion-weighted image was normalized by its own reference image prior to tensor fitting. To improve robustness, iteratively reweighted least squares fitting with outlier rejection (in the form of RESTORE (Chang et al., 2005) from the Camino toolkit (Cook et al., 2006)) was used to estimate tensors on a voxel-wise basis. Note that the RESTORE processing removes outlier gradients during the fitting process, but the number of removed data points varies by spatial location and scan. The quality assurance reports were visually examined to assess for motion/artifact, corrupted scans or other acquisition abnormalities and excluded subjects who had more than 5 corrupted volumes per scan. Additionally, all quantitative quality metrics were exported and outliers (>2 standard deviations) were visually assessed to identify processing failures. In total, there were 1404 sessions with two diffusion tensor imaging acquisitions. Quality assurance review identified concerns for 20 sessions, and these sessions were removed from further analyses, leaving 1384 good quality DTI sessions for analysis.

2.5. White matter regions of interest

To segment white matter regions of interest (ROIs), the Eve white matter atlas (Mori et al., 2008a,b) was combined with corresponding white matter labels from a multi-atlas segmentation using 35 manually labeled atlases from NeuroMorphometrics with the BrainCOLOR protocol (Klein et al., 2010), and FA mapped MRI. The white matter labels were intersected with the white matter segmentation and the resultant labels were iteratively grown to fill the remaining white matter space from the multi-atlas labels. The white matter ROI labels obtained from the T1-weighted image for each visit were affine registered to the

FA and MD images and used to extract average FA and MD values for each ROI. Fig. 1 shows the 16 ROIs used.

The ROIs investigated here were chosen based on findings related to the effects of vascular risk factors on regional white matter microstructure described in the introduction. These include eight association white matter ROIs: Superior longitudinal fasciculus (SLF), superior fronto-occipital fasciculus (SFO), inferior fronto-occipital fasciculus (IFO), sagittal stratum (SS), cingulum gyrus (CGC), cingulum (hippocampus) (CGH), fornix/stria terminalis (FX/ST), and the column and body of the fornix (FX); three commissural white matter ROIs: genu of the corpus callosum (GCC), body of the corpus callosum (BCC), and the splenium of the corpus callosum (SCC); and five projection white matter ROIs: anterior corona radiata (ACR), superior corona radiata (SCR), posterior corona radiata (PCR), anterior limb of the internal capsule (ALIC) and the posterior limb of the internal capsule (PLIC). FA and MD values from all ROIs were averaged across left and right hemispheres. Reliability of DTI measures has been established by many studies (Bonekamp et al., 2007; Pfefferbaum et al., 2003; Vollmar et al., 2010). Using the approach and Eve atlas ROIs implemented in the current analyses, we previously reported mean intraclass correlations (ICC) of 0.76 for FA and 0.66 for MD in aging adults in the BLSA (Venkatraman et al., 2015).

2.6. Statistical analysis

Prior to longitudinal modeling, intraclass correlations (ICCs) were used to assess the stability of DTI measures over time within each white matter ROI. Longitudinal trajectories in DTI metrics within all ROIs were analyzed using linear mixed effects models (LME). An initial base model was used to assess the effects of age and sex on longitudinal trajectories of DTI measures. The predictors included mean-centered age at baseline DTI visit, sex (male vs. female), race (non-white vs. white), scanner (scanner one and two vs. scanner three), time (follow up time in years since baseline), age*time, and sex*time. In model one, the effects of the vascular burden (model 1a), individual vascular risk factors (models 1b-1f), and *APOE* ε4 carrier status (carrier vs. non-carrier) (model 1g) were analyzed separately by adding the factor of interest and its time interaction to the base model. Model two included both vascular burden score and *APOE* ε4 to assess the independent effects of each predictor, while controlling for the other. We also assessed the following additional interactions: vascular burden**APOE* ε4 and vascular burden**APOE* ε4*time. As this analysis was exploratory, we did not correct for multiple comparisons in our analysis and report all results as significant at $p < 0.05$. However, we also indicate when results were significant at a more stringent value of $p < 0.01$. Effect sizes for the baseline cross-sectional effects were computed by dividing the beta coefficients by the standard deviation of baseline data, and effect sizes for the longitudinal effects were computed by dividing beta coefficients by the standard deviation of longitudinal rates of change. It should be noted that for vascular burden, the effect size represents the effect of one-unit change in the burden score, i.e. the effect for each additional vascular risk factor. All LME models were conducted using the lme function from the nlme package in R (Bates, 2007).

3. Results

3.1. Sample characteristics

Table 1 shows sample characteristics at baseline. On average, participants were 71.3 years old (SD = 9.9, range = 50–95), 56.7% were female, and 23.6% were *APOE* ε4 carriers. The average DTI follow-up period was 3.6 years (SD = 1.7, range = 0–8.3). Prevalence of each vascular risk factor is shown in Table 1 along with the distribution of the vascular burden score.

3.2. Cross-sectional analysis at baseline

3.2.1. Age and sex—Fig. 2 shows results from the base model, older baseline age was significantly associated with lower FA in all ROIs ($p < 0.001$) except the PCR and PLIC. Older age was also significantly associated with higher MD in all ROIs $p < 0.001$; Supplementary Table 1). Significant effects of sex showed that men compared with women had significantly higher FA in the SFO, IFO, CGC, FX/ST, GCC, BCC, ACR, SCR, ALIC, and the PLIC (*p- value range:* < 0.001–0.016). Men also showed significantly lower MD in the SLF, SFO, IFO, SS, CGC, GCC, ACR and the PLIC (*p-value range:* < 0.001–0.030). Results are shown in Supplementary Table 1.

3.2.2. Vascular burden and vascular risk factors—In model 1a, at baseline, the vascular burden score was significantly associated with lower FA in the SLF, SS, FX/ST, FX, GCC, BCC, SCC, ACR and the ALIC (*p-value range:* < 0.001–0.035). The vascular burden score was also significantly associated with higher MD in the SLF, SFO, GCG, FX, BCC, ACR, SCR, and the PLIC (*p-value range:* 0.001 – 0.046). These results are shown in Table 2 and represented in Fig. 3a.

Associations from models 1b—1f, between individual vascular risk factors and baseline FA and MD are shown in Supplementary Table 2. Hypertension was associated with lower FA in the FX/ST, FX, GCC, BCC, SCC and the ACR (*p-value range:* 0.009–0.035) at baseline. Hypertension was also associated with higher MD in the SLF, SFO, GCC, BCC, and the PLIC (*p-value range:* 0.005–0.048). Obesity was associated with lower baseline FA in the SLF, IFO, SS, FX/ST, BCC, SCC, ACR, and the ALIC (*p- value range:* < 0.001–0.047). Obesity was also associated with higher MD in the SLF, SFO, SS, CGC, BCC, ACR, SCR, and the PCR (*p-value range:* 0.002–0.034). Total cholesterol was associated with lower FA in the SCR ($p = 0.049$) but was not associated significantly with MD at baseline. Diabetes was not significantly associated with baseline FA or MD. Smoking status was associated with lower baseline FA in the FX/ST ($p = 0.020$) and FX ($p = 0.008$) and higher MD in the FX ($p = 0.045$).

3.2.3. APOE ε4—In model 1g, APOE ε4 carriers did not show any significant differences in FA or MD at baseline when compared to non-carriers except for higher MD in the SS ($p = 0.023$, Table 2).

3.2.4. Vascular burden and APOE ε4 status and their interaction—In model 2, when *APOE* ε4 status was also included in the model, the associations between the vascular

burden score and DTI metrics were largely unchanged although significant associations between FA and the vascular burden score were lost for the FX/ST and the SCC. Additionally, the association between MD in the SFO, FX, and ACR were no longer significant (Table 3). The significant association between APOE ε4 carrier status and MD in the SS observed in Model 1g was lost in model 2 after controlling for vascular burden, however a significant negative association between MD in the CHG and *APOE* ε4 emerged ($p = 0.041$). There were no significant associations for the vascular burden*APOE ε4 interaction at baseline for FA or MD.

3.3. Longitudinal analysis

3.3.1. Time effect—The median ICC for FA and MD across all regions was 0.764, indicating acceptable levels of test-retest stability in these metrics across white matter ROIs. In the base model, FA showed significant rates of decline over time in all ROIs (p 0.001), except the SLF, GCC and PLIC. MD showed significant rates of increase over time in all ROIs (p 0.001), except the GCC (Fig. 2 & Supplementary Table 1).

3.3.2. Age*time and Sex*time—In the base model, older baseline age was associated with greater decreases in FA in the FX/ST ($p = 0.026$), older baseline age was also associated with greater increases in MD in the SLF, SFO, IFO, SS, FX/ST, ACR, SCR, PCR, ALIC, and PLIC (*p-value range:* 0.001 – 0.043). Women showed greater decreases in FA in the CGC ($p = 0.006$). For MD, men showed greater increases in the GCC ($p = 0.008$). Results are shown in Supplementary Table 1.

3.3.3. Vascular burden*time and vascular risk factors*time—In model 1a, higher vascular burden score was associated with greater decline in FA in the CGH ($p = 0.003$), FX/ST ($p = 0.036$) and the SCC ($p = 0.045$). Higher vascular burden scores were also associated with greater increases in MD in the SCC ($p = 0.002$), as shown in Table 4 and Fig. 3b.

In models 1b-1f, the effects of baseline individual vascular risk factors on the rates of change in FA and MD are shown in Supplementary Table 3. Hypertension was not associated significantly with rates of change in FA but was associated with greater increases in MD in the CGH ($p = 0.023$) and the SCC ($p = 0.041$). Obesity was associated with greater decreases in FA in the SFO ($p = 0.025$), SCR ($p = 0.003$), and the PCR ($p = 0.017$) but was not associated with rates of change of MD. Cholesterol was associated with greater increases in FA in the ACR ($p = 0.037$) and the SCR ($p = 0.018$), but was not associated with rates of change of MD. Diabetes was not associated with rates of change in FA but was associated with greater increases in MD in the ACR ($p = 0.007$). Smoking was not associated with rates of change in FA or MD.

3.3.4. APOE ε4*time—In model 1b, *APOE* ε4 carriers compared with non-carriers had significantly greater decline in FA in the GCC ($p = 0.01$) and the SCC ($p = 0.022$) but did not differ in rates of change in MD (Fig. 3b, Table 4).

3.3.5. Vascular Burden*time and APOE ε4*time and their interaction—Associations between vascular burden and DTI metrics remained significant after

controlling for *APOE* ε4 status (Model 2) except for the effect on FA in the SCC. The significant association between *APOE* ε4 status and FA in the SCC observed in Model 1b was lost when controlling for vascular burden in model 2. There were no associations found for the interaction vascular burden*APOE ε4*time, except for greater decline in FA in the SCR ($p = 0.048$) and greater decline in MD in the FX in *APOE* ε4 carriers with greater vascular burden ($p = 0.008$). Results are shown in Table 5.

4. Discussion

The primary aims of this study were to investigate the impact of a cumulative vascular burden score, individual vascular risk factors, and APOE ε4 carrier status on white matter microstructural degeneration in a large sample of cognitively normal older adults. We also examined the effects of age and sex on DTI metrics. In addition to the expected decline in FA and increase in MD with age and the passage of time, we found that increased vascular burden was associated with reduced FA and increased MD at baseline and with faster rates of change over time in limbic and commissural white matter ROIs. Furthermore, APOE ε4 status predicted faster rates of decline in FA in anterior and posterior portions of the corpus callosum. Finally, men compared to women had higher levels of microstructural organization cross-sectionally but showed inconsistent differences in longitudinal change.

4.1. Vascular burden and individual vascular risk factors

The cumulative vascular burden score was associated with lower baseline FA and higher MD in a range of white matter regions. These areas included ROIs involving association fibers connecting the frontal, occipital, temporal and parietal lobes (SLF, SFO, and SS), fibers within the limbic system (FX/ST, and FX body), commissural fibers (GCC, BCC, and SCC) and projection fibers (ACR, SCR, ALIC and PLIC). In the longitudinal analysis the vascular burden score was associated with greater decline in microstructure in the limbic system (CHG, and FX/ST) and part of the corpus callosum (SCC). The widespread effect of vascular burden on white matter microstructure at baseline is supported by previous reports that similar summary scores of vascular risk factors, such as metabolic syndrome or the Framingham Stroke Risk Profile, are associated with multiple white matter regions (Alfaro et al., 2018; Segura et al., 2009; Shimoji et al., 2013; Uiterwijk et al., 2018). Furthermore, lower FA in the Cingulum and Fornix and has previously been shown in MCI and AD patients compared to controls (Bozoki et al., 2012; Mielke et al., 2012). There is also evidence that the accumulation of multiple vascular risk factors elevates the risk developing AD (Luchsinger et al., 2005). Therefore, targeting vascular risk factors for early intervention in cognitively normal adults may prevent or slow this decline in white matter microstructure and prevent or delay the onset of clinical symptoms.

Previous longitudinal results are more limited. Bender and Raz (2015) found that vascular risk was associated with greater change in FA in the body of the corpus callosum and the dorsal cingulum over 2-year follow-up. In a subsequent analysis over a follow-up period of up to seven years in 38 adults (Bender et al., 2016), did not assess multiple vascular risk factors, but did examine the effect of hypertension on white matter microstructure and found no significant relationships with longitudinal change. We found that obesity and

hypertension were the two risk factors associated with the largest number of white matter ROIs at baseline and appeared to drive the associations with vascular burden score in our data. Similar relationships have been reported in previous studies, although these tend to be in studies with relatively small sample sizes compared to the present study or include younger participants (Karlsson et al., 2013; Maillard et al., 2012; McEvoy et al., 2015; Papageorgiou et al., 2017). However, two cross-sectional studies of aging reported that hypertension exacerbates the effects of aging on white matter microstructure in posterior white matter regions (temporal and occipital lobes) (Kennedy and Raz, 2009a,b), and that increased mean arterial blood pressure is associated with reduced FA in multiple white matter regions, even in normotensive participants (Salat et al., 2012).

We found that diabetes was not related to white matter microstructure in many ROIs, although it was related to faster increases in MD in the ACR over time. There were no significant relationships between diabetes and FA. This finding contrasts with other studies that have found reduced FA in subjects with diabetes compared to healthy controls (Hoogenboom et al., 2014; Hsu et al., 2012; Reijmer et al., 2013). One reason for the difference between studies may be that there was only a small percentage of participants with diabetes in the BLSA DTI sample (9%). The effect of elevated total cholesterol was also limited, with decreased FA in the SCR at baseline, but slower rates of change in FA in the ACR and SCR over time suggesting a positive effect of total cholesterol on longitudinal change in FA. However, there is cross-sectional evidence that higher cholestrol is associated with poorer white matter microstructure (Williams et al., 2013). Smoking also showed a limited impact on white matter microstructure in this study.

4.2. APOE ε4

We found no effect of APOE ε4 on FA or MD at baseline except for elevated MD in the SS. While Honea et al. (2009) also reported a limited impact of APOE ε4 on white matter microstructure located in the para-hippocampal gyrus, Patel et al. (2013) found no differences between *APOE* ε4 carriers and non-carriers. In our longitudinal analysis, we found that APOE ε4 carriers exhibited faster rates of decline in FA in the GCC and the SCC. However, when we controlled for vascular burden the association with FA in the SCC was lost. As APOE ε4 is associated with cardiovascular disease (Song et al., 2004) it is possible that the effect is due to vascular damage in the SCC. However, as the vascular burden effect on FA in the SCC was also lost in model 2, and given the small changes in the beta values between models 1a/lg and model 2, it is more likely that the loss of significance is due to statistical power constraints as a result of adding more covariates and three-way interactions rather than showing a true mediation effect. de Groot et al. (2015) found faster increases in FA in carriers compared to non-carriers in the centrum semi-ovale and lower global MD in carriers compared to non-carriers. The authors suggested that this counterintuitive effect may be due to a short follow-up and limited power for longitudinal analyses. With a longer follow-up time, we found that APOE ε4 carriers exhibited faster rates of decline in FA in the GCC and the SCC. The same pattern of reduced FA in the GCC and SCC while the BCC is spared has also been reported in MCI and AD patients compared to cognitively normal controls (Di Paola et al.,2010). Therefore, we may be observing early increases in the rate of change in the CC microstructure associated with increased risk of AD. The finding that

APOE ε4 status was not associated with DTI metrics in more white matter ROIs is consistent with the minimal associations found by others (Honea et al., 2009; Patel et al., 2013). The lack of associations with APOE ε4 status may also be due to the fact that our study focused on cognitively normal individuals. For example, in studies of regional GM atrophy related to APOE ε4 status, widespread associations are found in AD patients with APOE ε4 alleles (Bigler et al., 2000; Geroldi et al., 1999) but associations are less consistent in cognitively normal adults (Cherbuin et al., 2008; Den Heijer et al., 2002; Reiman et al., 1998). Further studies examining the dose effect of the ε4 allele (i.e. having one or two) may provide more insight in the impact of the APOE ε4 allele in a larger sample.

4.3. Sex differences

We found baseline sex differences that agree with and extend the findings of several reports of sex differences in white matter micro-structure in which men show higher levels of FA in regions including the corpus callosum, cingulum and frontal white matter (Menzler et al., 2011; Oh et al., 2007; Szeszko et al., 2003). In the longitudinal analysis, we found evidence for greater decline in FA in women compared to men in the CGC, but conversely observed greater increases in MD in men within the GCC. This contrasts with Sexton et al. (2014) who reported no sex differences in the rate of change in FA or MD in voxel-wise analysis using Tract-Based Spatial Statistics of healthy participants over a wider age range. Sexual dimorphisms in the white matter appear during puberty and are thought to be moderated by sex hormones. Boys show steeper increases in white matter volume while girls show less steep age-related increases (De Bellis et al., 2001; Lenroot et al., 2007; Perrin et al., 2008), and boys have higher FA and lower MD than girls in a wide range of white matter regions (Herting et al., 2012). In boys, testosterone predicts white matter microstructure while in girls, estradiol is associated with FA of the white matter (Herting et al., 2012). While the baseline sex differences we report are consistent with sex differences earlier in life, the longitudinal results are less clear, and more work is required to understand how sex may play a role in age-related white matter micro-structural decline.

4.4. Age

As with previous studies (Barrick et al., 2010; Charlton et al., 2006; Kennedy and Raz, 2009a,b; Salat et al., 2005; Sexton et al., 2014), we found widespread effects of age on white matter microstructure. Age was the strongest predictor of FA and MD. Older baseline age was not associated with greater rates of change in FA. However, we did find that older baseline age was associated with greater increases in MD in several white matter regions. This contrasts with Sexton et al. (2014) who reported faster rates of decline in FA and increases in MD associated with increasing age in voxel wise analysis. Despite the strong effects of age on baseline white matter microstructure, the effects of vascular burden remained significant in models controlling for age. This suggests that minimizing vascular burden in older individuals could be protective against white matter microstructural damage.

4.5. Limitations

The results of this study should be considered with some limitations in mind. While we sought to investigate the impact of various cardio-vascular risk factors on white matter microstructure, it should be noted that participants in the BLSA benefit from close medical

observation during the study, and therefore diseases such as diabetes and hypertension tend to be detected and treated promptly. As such, treatment effects in this cohort may be a confound and the effects of these cardiovascular risk factors on white matter microstructure may, in fact, be more severe in other populations. Furthermore, the mean age at baseline in our sample was relatively old (71.3 years), and it is well established that mid-life vascular risk factors can have a negative impact on white matter earlier in life (Debette et al., 2011; Knopman et al., 2011; Vuorinen et al.,2011). This may explain why we observed more wide spread effects at baseline compared to longitudinal analysis as the baseline effects may reflect damage that was already present and the longitudinal changes may reflect more subtle ongoing damage associated with vascular risk factors in later life.

Due to the large DTI data set analyzed, we used an atlas-based approach to extract regionally specific DTI metrics using the state-of-the-art Eve white matter atlas (Mori et al., 2008a,b) for this exploratory analysis. However, DTI tractography methods have the potential to produce more accurate, subject-specific renderings of white matter tracts. Our findings will guide selection of a smaller number of regions of interest to apply tractography in future work and explore the impact of vascular burden and APOE on DTI metrics in greater detail. Tract based spatial statistics (Smith et al., 2006) also offer a way of conducting voxel-wise analysis that would be complimentary to the work presented here and could be used to confirm our findings. In the present analysis, we did not include white matter hyperintensities (WMH) as a dependent variable or a covariate in our models. While microstructural decline as measured by DTI is highly related to macrostructural damage as measured by the extent of WMH (Seiler et al., 2018), future work should asses the relationships between the regional distribution of WMH and the risk factors assessed here. In this study, we treated the analysis as exploratory and did not correct for multiple comparisons when looking at associations across 16 ROIs as DTI metrics across ROIs that are highly intercorrelated. We acknowledge that this may increase the risk of type I errors but believe the use of a less stringent significance threshold identifies relationships of interest for future research.

4.6. Conclusions

In conclusion, in a large longitudinal cohort of cognitively normal older adults, we found that higher vascular burden is associated with diffuse white matter microstructural decline and faster rates of decline in temporal lobe and commissural white matter regions. These findings suggest that interventions designed to lower vascular burden in older individuals may have a positive impact on white matter microstructure integrity which could decrease the risk of cognitive impairment. Future work should assess the longitudinal associations between changes in white matter microstructure and decline in cognition and how risk factors may mediate such associations. The recent report of a 19% reduction in MCI and decreased white matter damage following intensive blood pressure lowering in the SPRINT-MIND trial is encouraging in this regard (Nasrallah, 2018; Williamson, 2018).

Supplementary Material

Refer to Web version on PubMed Central for supplementary material.

Acknowledgements

This research was supported by the Intramural Research Program of the National Institute on Aging, National Institutes of Health. We thank the staff of the BLSA and the NIA MRI facility for their assistance and the BLSA participants for their dedication to this study.

References

Alexander DC, Pierpaoli C, Basser PJ, Gee JC, 2001 Spatial transformations of diffusion tensor magnetic resonance images. IEEE Trans. Med. Imag. 20 (11). 1131–1139.

Alfaro FJ, Gavrieli A, Saade-Lemus P, Lioutas V-A, Upadhyay J, Novak V, 2018 White matter microstructure and cognitive decline in metabolic syndrome: a review of diffusion tensor imaging. Metab. Clin. Exp. 78, 52–68. [PubMed: 28920863]

Alves GS, Sudo FK, Alves C. E.d. O., Ericeira-Valente L, Moreira DM, Engelhardt E, Laks J, 2012 Diffusion tensor imaging studies in vascular disease: a review of the literature. Dementia & Neuropsychologia 6 (3), 158–163. [PubMed: 29213790]

>American Psychiatric Association, 1987 Diagnostic and Statistical Manual of Mental Health Disorders (DSM-III-R). American Psychiatric Association.

Barrick TR, Charlton RA, Clark CA, Markus HS, 2010 White matter structural decline in normal ageing: A prospective longitudinal study using tract-based spatial statistics. Neuroimage 51 (2), 565–577. 10.1016/j.neuroimage.2010.02.033. [PubMed: 20178850]

Basser PJ, Mattiello J, LeBihan D, 1994 MR diffusion tensor spectroscopy and imaging. Biophys. J. 66 (1), 259–267. 10.1016/S0006-3495C(94)80775-1. [PubMed: 8130344]

Bates D, 2007 nlme: Linear and Nonlinear Mixed Effects Models. R package version, pp. 31–128.

Bender AR, Raz N, 2015 Normal-appearing cerebral white matter in healthy adults: mean change over 2 years and individual differences in change. Neurobiol. Aging 36 (5), 1834–1848. [PubMed: 25771392]

Bender AR, Völkle MC, Raz N, 2016 Differential aging of cerebral white matter in middle-aged and older adults: a seven-year follow-up. Neuroimage 125, 74–83. [PubMed: 26481675]

Bendlin BB, Fitzgerald ME, Ries ML, Xu G, Kastman EK, Thiel BW, Johnson SC, 2010 White matter in aging and cognition: a cross-sectional study of microstructure in adults aged eighteen to eighty-three. Dev. Neuropsychol. 35 (3), 257–277. [PubMed: 20446132]

Bigler ED, Lowry CM, Anderson CV, Johnson SC, Terry J, Steed M, 2000 Dementia, quantitative neuroimaging, and apolipoprotein E genotype. Am. J. Neuroradiol. 21 (10), 1857–1868. [PubMed: 11110538]

Bonekamp D, Nagae LM, Degaonkar M, Matson M, Abdalla WMA, Barker PB, Horska A, 2007 Diffusion tensor imaging in children and adolescents: Reproducibility, hemispheric, and age-related differences. Neuroimage 34 (2), 733–742. 10.1016/j.neuroimage.2006.09.020. [PubMed: 17092743]

Bozoki AC, Korolev IO, Davis NC, Hoisington LA, Berger KL, 2012 Disruption of limbic white matter pathways in mild cognitive impairment and Alzheimer's disease: A DTI/FDG-PET Study. Hum. Brain Mapp. 33 (8), 1792–1802. [PubMed: 21674695]

Chang LC, Jones DK, Pierpaoli C, 2005 RESTORE: robust estimation of tensors by outlier rejection. Magn. Reson. Med.: An Official Journal of the International Society for Magnetic Resonance in Medicine 53 (5), 1088–1095.

Charlton RA, Barrick TR, McIntyre DJ, Shen Y, O'Sullivan M, Howe FA, Markus HS, 2006 White matter damage on diffusion tensor imaging correlates with age-related cognitive decline. Neurology 66 (2), 217–222. 10.1212/01.wnl.0000194256.15247.83. [PubMed: 16434657]

Charlton RA, Schiavone F, Barrick TR, Morris RG, Markus HS, 2010 Diffusion tensor imaging detects age related white matter change over a 2 year follow-up which is associated with working memory decline. J. Neurol. Neurosurg. Psychiatr. 81 (1), 13–19. 10.1136/jnnp.2008.167288.

Cherbuin N, Anstey KJ, Sachdev PS, Maller JJ, Meslin C, Mack HA, Easteal S, 2008 Total and regional gray matter volume is not related to APOE* ε4 status in a community sample of middle-

aged individuals. The Journals of Gerontology Series A: Biological Sciences and Medical Sciences 63 (5), 501–504. [PubMed: 18511754]

Cook P, Bai Y, Nedjati-Gilani S, Seunarine K, Hall M, Parker G, Alexander DC, 2006 Camino: open-source diffusion-MRI reconstruction and processing. In: Paper presented at the 14th scientific meeting of the international society for magnetic resonance in medicine.

De Bellis MD, Keshavan MS, Beers SR, Hall J, Frustaci K, Masalehdan A, Boring AM, 2001 Sex differences in brain maturation during childhood and adolescence. Cerebr. Cortex 11 (6), 552–557.

de Groot M, Cremers LG, Ikram MA, Hofman A, Krestin GP, van der Lugt A, Vernooij MW, 2015 White matter degeneration with aging: longitudinal diffusion MR imaging analysis. Radiology 279 (2), 532–541. [PubMed: 26536311]

Debette S, Seshadri S, Beiser A, Au R, Himali JJ, Palumbo C, DeCarli C, 2011 Midlife vascular risk factor exposure accelerates structural brain aging and cognitive decline. Neurology 77 (5), 461–468. 10.1212/WNL.0b013e318227b227. [PubMed: 21810696]

Den Heijer T, Oudkerk M, Launer L, Van Duijn C, Hofman A, Breteler M, 2002 Hippocampal, amygdalar, and global brain atrophy in different apolipoprotein E genotypes. Neurology 59 (5), 746–748. [PubMed: 12221169]

Di Paola M, Spalletta G, Caltagirone C, 2010 In vivo structural neuroanatomy of corpus callosum in Alzheimer's disease and mild cognitive impairment using different MRI techniques: a review. J. Alzheim. Dis. 20 (1), 67–95.

Geroldi C, Pihlajamäki M, Laakso MP, DeCarli C, Beltramello A, Bianchetti A, Frisoni GB, 1999. APOE-ε4 is associated with less frontal and more medial temporal lobe atrophy in AD. Neurology 53 (8), 1825 10.1212/wnl.53.8.1825,1825. [PubMed: 10563634]

Gottesman RF, Schneider AL, Zhou Y, Coresh J, Green E, Gupta N, Sharrett AR,2017 Association between midlife vascular risk factors and estimated brain amyloid deposition. J. Am. Med. Assoc. 317 (14), 1443–1450.

Herting MM, Maxwell EC, Irvine C, Nagel BJ, 2012 The Impact of Sex, Puberty, and Hormones on White Matter Microstructure in Adolescents. Cerebr. Cortex 22 (9), 1979–1992. 10.1093/cercor/bhr246.

Honea RA, Vidoni E, Harsha A, Burns JM, 2009 Impact of APOE on the healthy aging brain: a voxel-based MRI and DTI study. J. Alzheim. Dis. 18 (3), 553–564.

Hoogenboom WS, Marder TJ, Flores VL, Huisman S, Eaton HP, Schneiderman JS, Musen G, 2014 Cerebral White Matter Integrity and Resting-State Functional Connectivity in Middle-aged Patients With Type 2 Diabetes. Diabetes 63 (2), 728–738. 10.2337/db13-1219. [PubMed: 24203723]

Hsu J-L, Chen Y-L, Leu J-G, Jaw F-S, Lee C-H, Tsai Y-F, Leemans A, 2012 Microstructural white matter abnormalities in type 2 diabetes mellitus: a diffusion tensor imaging study. Neuroimage 59 (2), 1098–1105. [PubMed: 21967726]

Inano S, Takao H, Hayashi N, Abe O, Ohtomo K, 2011 Effects of Age and Gender on White Matter Integrity. Am. J. Neuroradiol. 32 (11), 2103–2109. 10.3174/ajnr.A2785. [PubMed: 21998104]

Karlsson HK, Tuulari JJ, Hirvonen J, Lepomäki V, Parkkola R, Hiltunen J, Salminen P, 2013 Obesity is associated with white matter atrophy: A combined diffusion tensor imaging and voxel-based morphometric study. Obesity 21 (12), 2530–2537. [PubMed: 23512884]

Kennedy KM, Raz N, 2009a Aging white matter and cognition: differential effects of regional variations in diffusion properties on memory, executive functions, and speed. Neuropsychologia 47 (3), 916–927. [PubMed: 19166865]

Kennedy KM, Raz N, 2009b. Pattern of normal age-related regional differences in white matter microstructure is modified by vascular risk. Brain Res. 1297, 41–56. 10.1016/j.brainres.2009.08.058. [PubMed: 19712671]

Klein A, Dal Canton T, Ghosh SS, Landman B, Lee J, Worth A, 2010 Open labels: online feedback for a public resource of manually labeled brain images. In: Paper presented at the 16th Annual Meeting for the Organization of Human Brain Mapping.

Knopman DS, Penman AD, Catellier DJ, Coker LH, Shibata DK, Sharrett AR, Mosley TH, 2011 Vascular risk factors and longitudinal changes on brain MRI. The ARIC study. 10.1212/WNL.0b013e31821d753f.

Lakatta EG, Levy D, 2003 Arterial and cardiac aging: major shareholders in cardiovascular disease enterprises: Part I: aging arteries: a “set up” for vascular disease. Circulation 107 (1), 139–146. [PubMed: 12515756]

Lauzon CB, Asman AJ, Esparza ML, Burns SS, Fan Q, Gao Y, Landman BA, 2013 Simultaneous analysis and quality assurance for diffusion tensor imaging. PLoS One 8 (4) e61737.

Lee DY, Fletcher E, Martinez O, 2009 Regional pattern of white matter microstructural changes in normal aging. MCI, and AD. Neurology 73.

Lenroot RK, Gogtay N, Greenstein DK, Wells EM, Wallace GL, Clasen LS, Evans AC, 2007 Sexual dimorphism of brain developmental trajectories during childhood and adolescence. Neuroimage 36 (4), 1065–1073. [PubMed: 17513132]

Luchsinger J, Reitz C, Honig LS, Tang M-X, Shea S, Mayeux R, 2005 Aggregation of vascular risk factors and risk of incident Alzheimer disease. Neurology 65 (4), 545–551. [PubMed: 16116114]

Maillard P, Seshadri S, Beiser A, Himali JJ, Au R, Fletcher E, DeCarli C, 2012 Effects of systolic blood pressure on white-matter integrity in young adults in the Framingham Heart Study: a cross-sectional study. Lancet Neurol. 11 (12), 1039–1047. [PubMed: 23122892]

McEvoy LK, Fennema-Notestine C, Eyler LT, Franz CE, Hagler DJ, Lyons MJ, Kremen WS, 2015 Hypertension-related alterations in white matter microstructure detectable in middle age. Hypertension, HYPERTENSIONAHA. 115, 05336.

McKhann G, Drachman D, Folstein M, Katzman R, Price D, Stadlan EM, 1984 Clinical diagnosis of Alzheimer’s disease Report of the NINCDS-ADRDA Work Group* under the auspices of Department of Health and Human Services Task Force on Alzheimer’s Disease. Neurology 34 (7), 939, 939. [PubMed: 6610841]

Menzler K, Belke M, Wehrmann E, Krakow K, Lengler U, Jansen A, Knake S, 2011 Men and women are different: Diffusion tensor imaging reveals sexual dimorphism in the microstructure of the thalamus, corpus callosum and cingulum. Neuroimage 54 (4), 2557–2562. 10.1016/j.neuroimage.2010.11.029. [PubMed: 21087671]

Mielke MM, Okonkwo OC, Oishi K, Mori S, Tighe S, Miller MI, et al., 2012 Fornix integrity and hippocampal volume predict memory decline and progression to Alzheimer’s disease. Alzheimer’s Dementia: The Journal of the Alzheimer’s Association 8 (2), 105–113. 10.1016/j.jalz.2011.05.2416.

Mori S, Oishi K, Jiang H, Jiang L, Li X, Akhter K, Woods R, 2008a Stereotaxic white matter atlas based on diffusion tensor imaging in an ICBM template. Neuroimage 40 (2), 570–582. [PubMed: 18255316]

Mori S, Oishi K, Jiang H, Jiang L, Li X, Akhter K, Mazziotta J, 2008b Stereotaxic white matter atlas based on diffusion tensor imaging in an ICBM template. Neuroimage 40 (2), 570–582. 10.1016/j.neuroimage.2007.12.035. [PubMed: 18255316]

Nasrallah IM, 2018 A randomized trial of intensive versus standard systolic blood pressure control on brain structure: results from sprint mind MRI. Alzheimer’s Dementia: The Journal of the Alzheimer’s Association 14 (7), P1666.

Nir TM, Jahanshad N, Villalon-Reina JE, Toga AW, Jack CR, Weiner MW, Initiative A.s.D.N., 2013 Effectiveness of regional DTI measures in distinguishing Alzheimer’s disease, MCI, and normal aging. Neuroimage: Clinica 3, 180–195.

Oh JS, Song IC, Lee JS, Kang H, Park KS, Kang E, Lee DS, 2007 Tractography-guided statistics (TGIS) in diffusion tensor imaging for the detection of gender difference of fiber integrity in the midsagittal and parasagittal corpora callosa. Neuroimage 36 (3), 606–616. 10.1016/j.neuroimage.2007.03.02. [PubMed: 17481923]

Ota M, Obata T, Akine Y, Ito H, Ikehira H, Asada T, Suhara T, 2006 Age-related degeneration of corpus callosum measured with diffusion tensor imaging. Neuroimage 31 (4), 1445–1452. 10.1016/j.neuroimage.2006.02.008. [PubMed: 16563802]

Papageorgiou I, Astrakas LG, Xydis V, Alexiou GA, Bargiotas P, Tzarouchi L, Argyropoulou MI, 2017 Abnormalities of brain neural circuits related to obesity: a diffusion tensor imaging study. Magn. Reson. Imag. 37, 116–121.

Patel KT, Stevens MC, Pearlson GD, Winkler AM, Hawkins KA, Skudlarski P, Bauer LO, 2013 Default mode network activity and white matter integrity in healthy middle-aged Apoε4 carriers. Brain Imaging and Behavior 7 (1), 6–67. 10.1007/s11682-012-9187-y.

Perrin JS, Herve P-Y, Leonard G, Perron M, Pike GB, Pitiot A, Paus T, 2008 Growth of white matter in the adolescent brain: role of testosterone and androgen receptor. J. Neurosci. 28 (38), 9519–9524. [PubMed: 18799683]

Petersen RC, 2004 Mild cognitive impairment as a diagnostic entity. J. Intern. Med. 256 (3), 183–194. [PubMed: 15324362]

Pfefferbaum A, Adalsteinsson E, Sullivan EV, 2003 Replicability of diffusion tensor imaging measurements of fractional anisotropy and trace in brain. J. Magn. Reson. Imag. 18 (4), 427–433. 10.1002/jmri.10377.

Pierpaoli C, Jezzard P, Basser PJ, Barnett A, Di Chiro G, 1996 Diffusion tensor MR imaging of the human brain. Radiology 201 (3), 637–648. [PubMed: 8939209]

Reijmer YD, Brundel M, De Bresser J, Kappelle LJ, Leemans A, Biessels GJ, Group UVCIS, 2013 Microstructural white matter abnormalities and cognitive functioning in type 2 diabetes: a diffusion tensor imaging study. Diabetes Care 36 (1), 137–144. [PubMed: 22961577]

Reiman EM, Uecker A, Caselli RJ, Lewis S, Bandy D, De Leon MJ, Weaver A, 1998 Hippocampal volumes in cognitively normal persons at genetic risk for Alzheimer's disease.: Ann. Neurol. Official Journal of the American Neurological Association and the Child Neurology Society 44 (2), 288–291.

Salat DH, Tuch DS, Greve DN, van der Kouwe AJW, Hevelone ND, Zaleta AK, Dale AM, 2005 Age-related alterations in white matter microstructure measured by diffusion tensor imaging. Neurobiol. Aging 26 (8), 1215–1227. 10.1016/j.neurobiolaging.2004.09.017. [PubMed: 15917106]

Salat DH, Williams VJ, Leritz EC, Schnyer DM, Rudolph JL, Lipsitz LA, Milberg WP, 2012 Inter-individual variation in blood pressure is associated with regional white matter integrity in generally healthy older adults. Neuroimage 59 (1), 181–192. 10.1016/j.neuroimage.2011.07.033. [PubMed: 21820060]

Segura B, Jurado M, Freixenet N, Falcon C, Junqué C, Arboix A, 2009 Microstructural white matter changes in metabolic syndrome A diffusion tensor imaging study. Neurology 73 (6), 438–444. [PubMed: 19667318]

Seiler S, Fletcher E, Hassan-Ali K, Weinstein M, Beiser A, Himali JJ, Maillard P, 2018 Cerebral tract integrity relates to white matter hyperintensities, cortex volume, and cognition. Neurobiol. Aging 72, 14–22. [PubMed: 30172922]

Sexton CE, Walhovd KB, Storsve AB, Tamnes CK, Westlye LT, Johansen-Berg H, Fjell AM, 2014 Accelerated Changes in White Matter Microstructure during Aging: A Longitudinal Diffusion Tensor Imaging Study. J. Neurosci. 34 (46), 15425–15436. 10.1523/jneurosci.0203-14.2014. [PubMed: 25392509]

Shimoji K, Abe O, Uka T, Yasmin H, Kamagata K, Asahi K, Watada H, 2013 White matter alteration in metabolic syndrome: diffusion tensor analysis. Diabetes Care 36 (3), 696–700. [PubMed: 23172976]

Shock NW, 1984 Normal human aging: The Baltimore longitudinal study of aging.

Smith SM, Jenkinson M, Johansen-Berg H, Rueckert D, Nichols TE, Mackay CE, Matthews PM, 2006 Tract-based spatial statistics: voxelwise analysis of multisubject diffusion data. Neuroimage 31 (4), 1487–1505. [PubMed: 16624579]

Song Y, Stampfer MJ, Liu S, 2004 Meta-analysis: apolipoprotein E genotypes and risk for coronary heart disease. Ann. Intern. Med. 141 (2), 137–147. [PubMed: 15262670]

Szeszko PR, Vogel J, Ashtari M, Malhotra AK, Bates J, Kane JM, Lim K, 2003 Sex differences in frontal lobe white matter microstructure: a DTI study. Neuroreport 14 (18), 2469–2473. [PubMed: 14663212]

Teipel SJ, Meindl T, Wagner M, Stieltjes B, Reuter S, Hauenstein K-H, Hampel H, 2010 Longitudinal changes in fiber tract integrity in healthy aging and mild cognitive impairment: a DTI follow-up study. J. Alzheim. Dis. 22 (2), 507–522.

Thom T, Haase N, Rosamond W, Howard VJ, Rumsfeld J, Manolio T, Wolf P, 2006 Heart Disease and Stroke Statistics—2006 Update. A Report From the American Heart Association Statistics

Committee and Stroke Statistics Subcommittee 113 (6), e85–e151. 10.1161/circulationaha.105.171600.

Tian Q, Ferrucci L, Resnick SM, Simonsick EM, Shardell MD, Landman BA, Studenski SA, 2016 The effect of age and microstructural white matter integrity on lap time variation and fast-paced walking speed. Brain Imaging and Behavior 10 (3), 697–706. [PubMed: 26399234]

Uiterwijk R, Staals J, Huijts M, de Leeuw PW, Kroon AA, van Oostenbrugge RJ,2018 Framingham Stroke Risk Profile is related to cerebral small vessel disease progression and lower cognitive performance in patients with hypertension. J. Clin. Hypertens. 20 (2), 240–245.

Venkatraman VK, Gonzalez CE, Landman B, Goh J, Reiter DA, An Y, Resnick SM, 2015 Region of interest correction factors improve reliability of diffusion imaging measures within and across scanners and field strengths. Neuroimage 119, 406–416. 10.1016/j.neuroimage.2015.06.078. [PubMed: 26146196]

Vollmar C, O'Muircheartaigh J, Barker GJ, Symms MR, Thompson P, Kumari V, Koepp MJ, 2010 Identical, but not the same: intra-site and inter-site reproducibility of fractional anisotropy measures on two 3.0 T scanners. Neuroimage 51 (4), 1384–1394. [PubMed: 20338248]

Vuorinen M, Solomon A, Rovio S, Nieminen L, Kåreholt I, Tuomilehto J, Kivipelto M, 2011 Changes in vascular risk factors from midlife to late life and white matter lesions: a 20-year follow-up study. Dement. Geriatr. Cognit. Disord. 31 (2), 119–125. [PubMed: 21273771]

Williams VJ, Leritz EC, Shepel J, McGlinchey RE, Milberg WP, Rudolph JL, Salat DH, 2013 Interindividual variation in serum cholesterol is associated with regional white matter tissue integrity in older adults. Hum. Brain Mapp. 34 (8), 1826–1841. [PubMed: 22438182]

Williamson JD, 2018 A Randomized Trial of Intensive Versus Standard Systolic Blood Pressure Control and the Risk of Mild Cognitive Impairment and Dementia: Results from SPRINT MIND. Alzheimer's Dementia: The Journal of the Alzheimer's Association 14 (7), P1665–P1666.

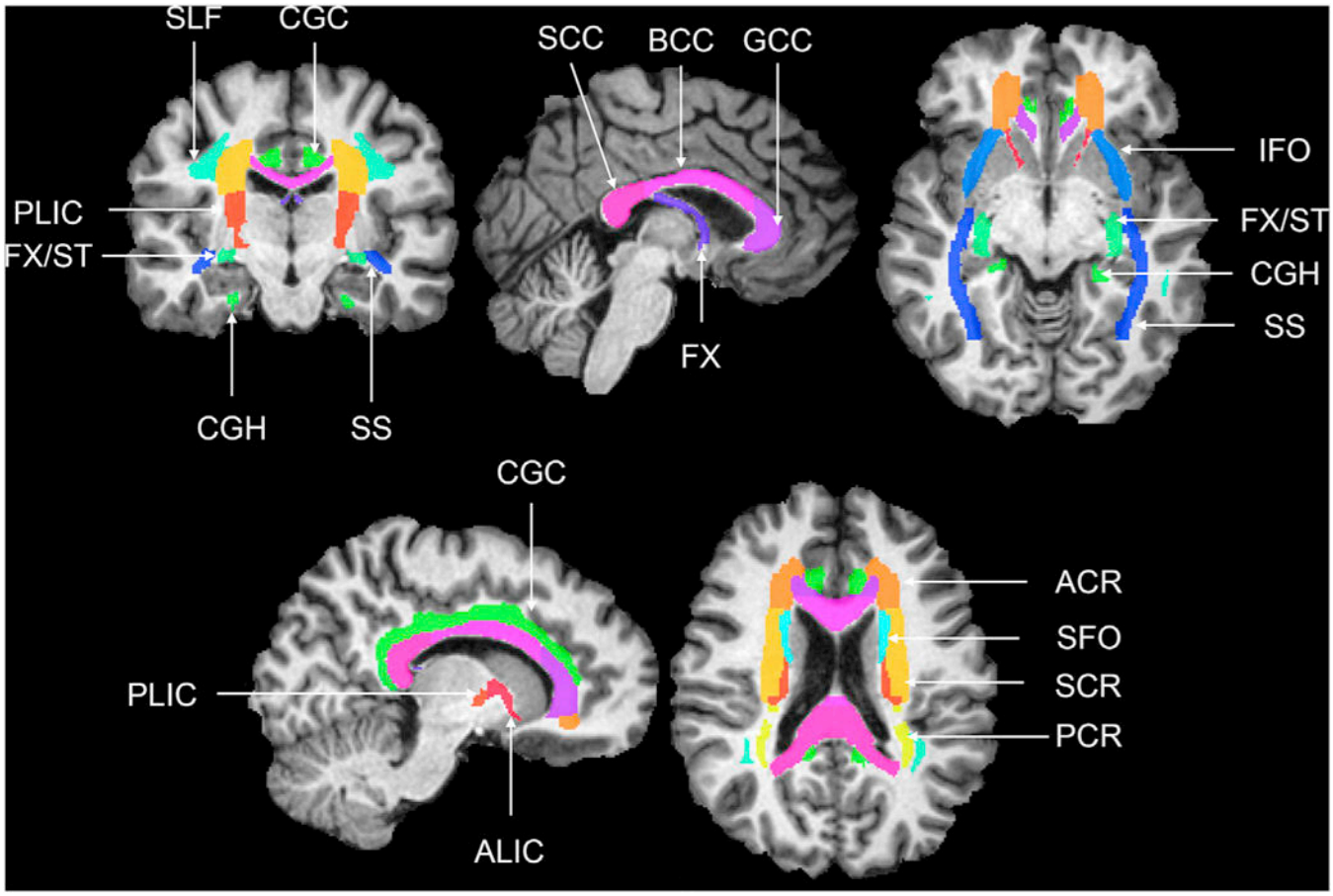

Fig. 1.

Coronal, axial and sagittal slices showing the Eve white matter ROIs (Mori et al., 2008a,b) over-laid on a T1-weighted image. anterior corona radiata (ACR), anterior limb of the internal capsule (ALIC), body of the corpus callosum (BCC), cingulum gyrus (CGC), cingulum (hippocampus) (CGH), column and body of the fornix (FX), fornix/stria terminalis (FX/ST), genu of the corpus callosum (GCC), inferior fronto-occipital fasciculus (IFO), posterior corona radiata (PCR), posterior limb of the internal capsule (PLIC), corpus callosum (SCC), superior corona radiata (SCR), superior fronto-occipital fasciculus (SFO), Superior longitudinal fasciculus (SLF), sagittal stratum (SS).

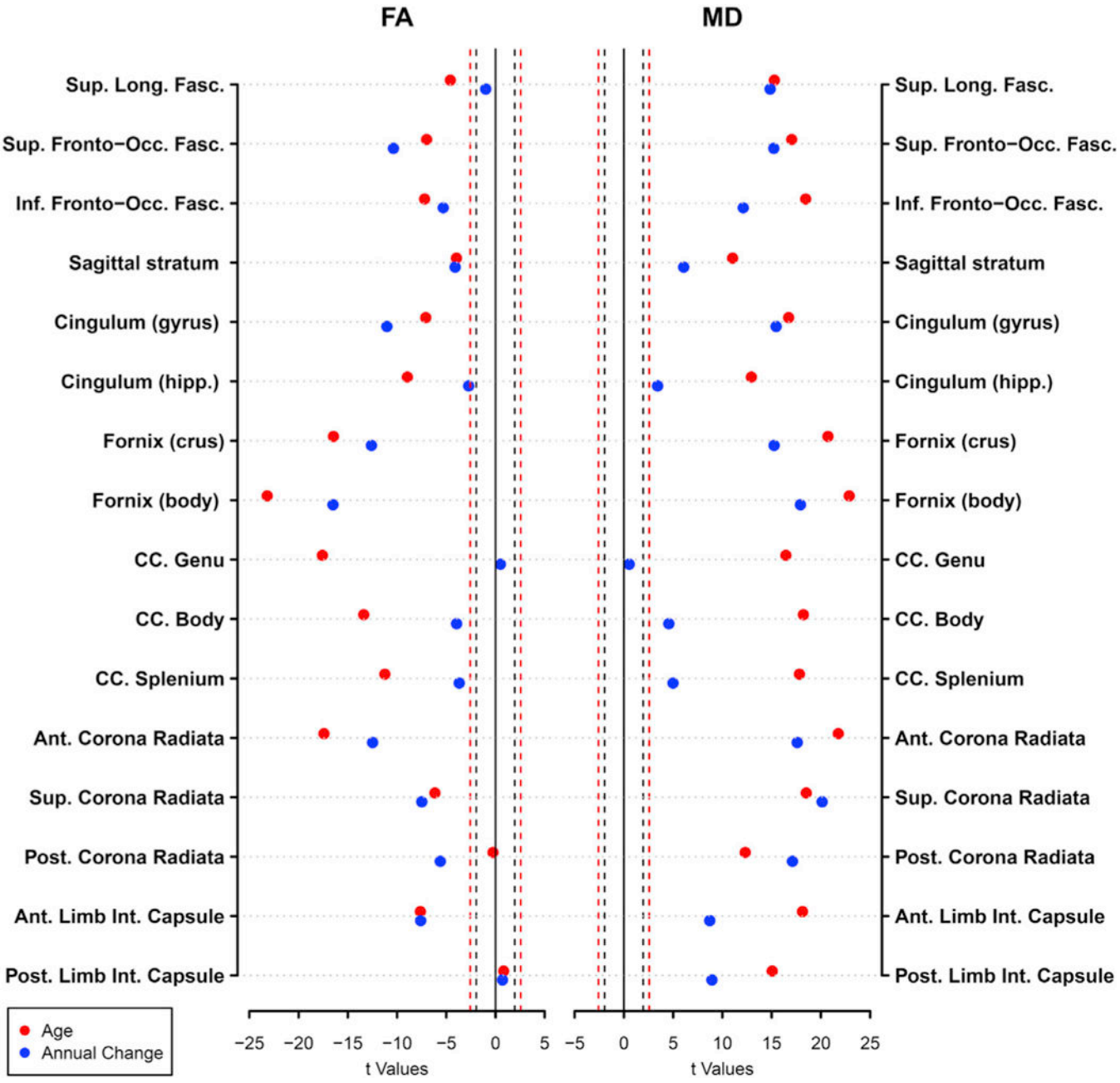

Fig. 2.

Dot plot showing the t-values from linear mixed effects analysis results for age (red) and annual rates of change (blue) on FA and MD. The dashed lines represent the thresholds for significance for $p = 0.05$ (black) and $p = 0.01$ (red). Moving from zero, points on the outside of the dashed lines represent significant effects. Covariates included sex, race, and scanner.

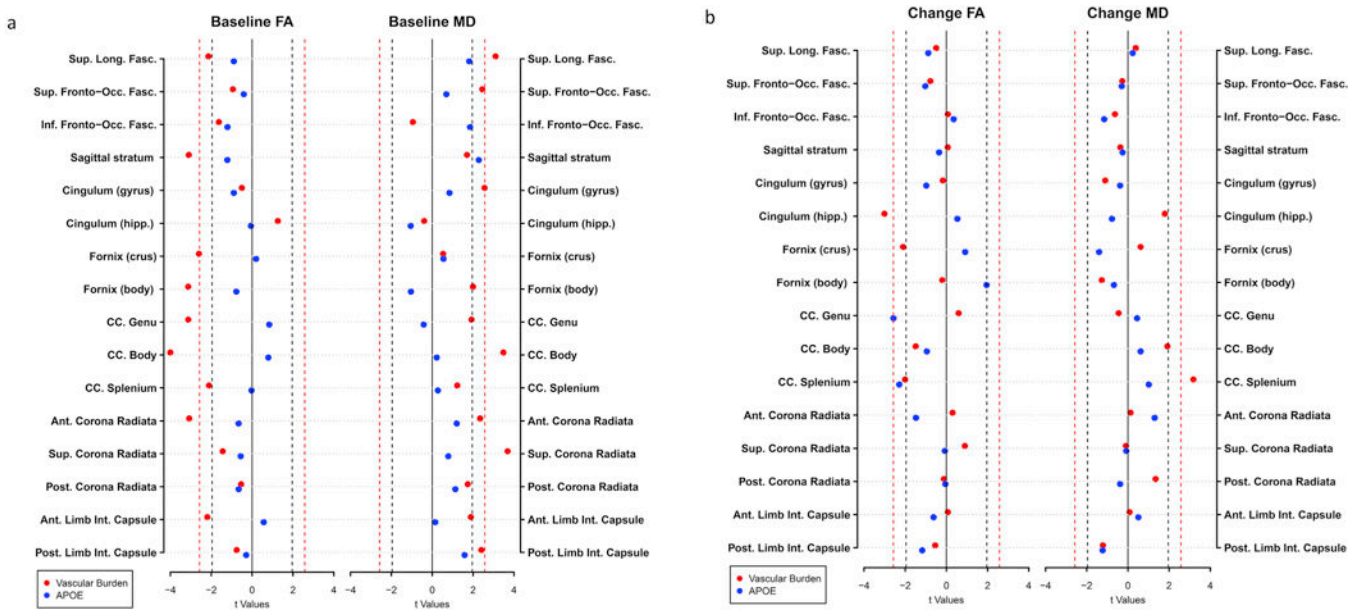

Fig. 3.

Dot plots showing the effects of the vascular burden (red) and having an APOE ε4 allele (blue) on (a) baseline FA and MD and (b) change in FA and MD. The dashed lines represent the thresholds for significance for $p = 0.05$ (black) and $p = 0.01$ (red). Moving from zero, points on the outside of the dashed lines represent significant effects. Covariates included age, sex, race, and scanner.

Table 1

Overall participant characteristics.

N Data Points	1384
N Subjects	665
N Subjects with Longitudinal DTI	406
Baseline Age, mean (SD)	71.3 (10.0)
range	50–95
Females, No. (%)	377 (56.7)
White, No. (%)	440 (66.2)
Education years, mean (SD)	17.0 (2.5)
range	7–24
APOE ε4 Carriers, No. (%)	157 (23.6)
Hypertension, No. (%)	306 (46.0)
Obese, No. (%)	150 (22.6)
Elevated Cholesterol, No. (%)	224 (33.7)
Diabetes, No. (%)	61 (9.2)
Smoking (current/ever vs. never), No. (%)	281 (42.3)
Vascular Burden, No. (%)	0 = 98 (14.7)
	1 = 236 (35.5)
	2 = 204 (30.7)
	3+ = 113 (17.0)
Follow-up Interval in years, mean (SD)	3.6 (1.7)
range	0–8.3
Number of Visits, mean (SD)	2.8 (1.0)
range	1–8

Table 2

Baseline associations between vascular burden and APOE ε4 status with DTI parameters Results are from separate models for each predictor variable, controlling for baseline age, sex, race, and scanner.

	FA						MD					
	Vascular Burden			APOE ε4			Vascular Burden			APOE ε4		
	Beta	95% C.I.	Effect Size[¥]	Beta	95% C.I.	Effect Size	Beta	95% C.I.	Effect Size[¥]	Beta	95% C.I.	Effect Size
Superior Longitudinal.Fasciculus	−0.0025[*]	−0.0048, −0.00022	−0.087	−0.0023	−0.0075, 0.0028	−0.08	4.10e-06[†]	1.5e-06, 6.8e-06	0.11	5.50e-06	−4.5e-07, 1.1e-05	−0.06
Sup. Franto-Occ. Fasc.	−0.0017	−0.0053, 0.0019	−0.04	−0.0016	−0.0096, 0.0063	−0.04	8.30e-06[*]	1.7e-06, 1.5e-05	0.08	5.30e-06	−9.7e-06, 2e-0S	−0.08
Int Pronto-Occ. Fasc.	−0.0017	−0.0038, 0.00035	−0.06	−0.0028	−0.0074, 0.0018	−0.10	−1.70e-06	−5.1e-06,1.8e-06	−0.03	7.20e-06	−4.3e-07, 1.5e-05	0.02
Sagittal stratum	−0.004[†]	−0.0065, −0.0015	−0.13	−0.0035	−0.0091, 0.0021	−0.11	2.60606	−4e-07, 5.6e-06	0.06	7.70e-06[*]	1.1e-06, 1Ae-05	−0.02
Cingulum (gyrus)	−0.00065	−0.0032, 0.0019	−0.02	−0.0026	−0.0081, 0.003	−0.08	3.30e-06[*]	7.8e-07, 5.9e-06	0.09	2.50e-06	−3.2e-06, 8.2e-06	−0.08
Cingulum (hipp.)	0.0021	−0.0012, 0.0054	0.05	−0.00022	−0.0076, 0.0071	0.00	−8.10e-07	−4.9e-06, 3.3e-06	−0.01	−4.90e-06	−1.4e-05, 4.2e-06	0.03
Fornix (crus)	−0.0025[*]	−0.0044, −0.00062	−0.09	0.00042	−0.0038, 0.0046	0.02	110606	−3.2e-06, 5.5e-06	0.02	2.70e-06	−6.9e-06, 1.2e-05	0.06
Fornix (body)	−00.0052020	−0.0082, −0.0019	−0.09	−0.0028	−0.0098, 0.0043	−0.05	150e-05[*]	2.8.07, 3e-05	0.06	−1.80e-OS	−5.1e-05, 1.6e-OS	0.16
CC. Genu	−0.0062[†]	−0.01, −0.0023	−0.11	0.0037	−0.005, 0.012	0.06	1.00e-05	−2e-07, 21e-05	0.06	−5,00e-06	−2.9e-05, 1.9e-05	−0.18
CC. Body	−0.0061[†]	−0.0091, −0.0031	−0.15	0.0027	−0.004, 0.0095	0.06	1.00e-05[†]	4.5e-06, 1.6.05	0.11	1.50e-06	−1.2e-0S, 1.5e-05	−0.07
CC. Splenium	−0.0026[*]	−0.005, −0.00019	−0.08	−7.30e-05	−0.0055, 0.0053	0.00	3.40e-06	−2.1e-06, 8.9e-06	0.04	1.70e-06	−le-OS, 1.4e-05	−0.15
Ant. Corona Radian	−0.0038f	−0.0062, −0.0014	−0.10	−0.0018	−0.0072, 0.0036	−0.05	4.40e-06[*]	7.1e-07, 8e-06	0.07	5.00e-06	−3.2e-06, 1.3.05	−0.12
Sup. Canna Radiant	−0.0018	−0.0044, 0.00067	−0.06	−0.0016	−0.0071, 0.0039	−0.05	6.20e-06[†]	2.9e-06, 9.4e-06	0.13	2.90e-06	−4.4e-06, 1e-05	−0.01
Post. Corona Radials	−0.00099	−0.0046, 0.0026	−0.02	−0.0027	−0.011, 0.0053	−0.06	3.60e-06	−4.5e-07, 7.6e-06	0.07	5.20e-06	−3.9e-06, 1.4e-05	0.00
Ant. Limb Int. Capsule	−0.0036[*]	−0.0068, −0.00038	−0.08	0.002	−0.0051, 0.0092	0.05	4.80e-06	−1.8e-07, 9.9e-06	0.06	8.30e-07	−1e-05, 1.2e-05	−0.04
Post. Limb Inc. Capsule	−0.00095	−0.0034, 0.0015	−0.03	−0.00081	−0.0063, 0.0046	−0.03	3.00e-06[*]	5.5e-07, 5.4e-06	0.08	4.40e-06	−1e-06, 9.8e-06	−0.08

[*] significant at $p < 0.05$.

[†] significant at $p < 0.01$.

[¥] Effect sizes represents the effect for one-unit change in vascular burden score.

Neuroimage. Author manuscript; available in PMC 2019 July 01.

Table 3

Baseline associations between vascular burden, APOE ε4 carrier status, and their interaction term with DTI parameters. Results are from the same model controlling for baseline age, sex, race, and scanner.

	FA								
	Vascular Burden			APOE ε4			Vascular Burden * APOE ε4		
	Beta	95% C.I.	Effect Size¥	Beta	95% C.I.	Effect Size	Beta	95% C.I.	Effect Size
Sup. Long. Fasc.	−0.0026*	−0.0052, −7.4e-06	−0.09	−0.0025	−0.012, 0.0073	−0.09	0.00015	−0.0054, 0.0057	0.01
Sup. Fronto-Occ. Fasc.	−0.00058	−0.0046, 0.0034	−0.01	0.0058	−0.0094, 0.021	0.13	−0.0055	−0.014, 0.0031	−0.12
Inf. Fronto-Occ. Fasc.	−0.0016	−0.004, 0.00074	−0.06	−0.002	−0.011, 0.0068	−0.07	−0.00066	−0.0056, 0.0043	−0.02
Sagittal stratum	−0.0039†	−0.0067, −0.0011	−0.12	−0.0034	−0.014, 0.0075	−0.11	−0.00025	−0.0063, 0.0058	−0.01
Cingulum (gyrus)	−0.00091	−0.0037, 0.0019	−0.03	−0.0043	−0.015, 0.0065	−0.13	0.001	−0.0051, 0.0071	0.03
Cingulum (hipp.)	0.0018	−0.0019, 0.0056	0.04	−0.0028	−0.017, 0.011	−0.06	0.0014	−0.0065, 0.0094	0.03
Fornix (crus)	−0.0019	−0.004, 0.00025	−0.07	0.0044	−0.0036, 0.012	0.16	−0.0027	−0.0072, 0.0018	−0.10
Fornix (body)	−0.0045*	−0.008, −0.00091	−0.08	0.001	−0.013, 0.015	0.02	−0.0027	−0.01, 0.005	−0.05
CC. Genu	−0.0067†	−0.011, −0.0023	−0.11	9.00e-04	−0.016, 0.018	0.02	0.0022	−0.0073, 0.012	0.04
CC. Body	−0.0065†	−0.0099, −0.0032	−0.15	−0.00059	−0.013, 0.012	−0.01	0.0023	−0.005, 0.0096	0.05
CC. Splenium	−0.0026	−0.0053, 8.7e-05	−0.08	−0.00039	−0.011, 0.01	−0.01	−0.00024	−0.0061, 0.0056	−0.01
Ant. Corona Radiata	−0.0037†	−0.0064, −0.001	−0.10	−0.0021	−0.012, 0.0082	−0.06	−0.00038	−0.0062, 0.0054	−0.01
Sup. Corona Radiata	−0.0018	−0.0046, 0.0011	−0.06	−0.0011	−0.012, 0.0095	−0.04	−0.00045	−0.0065, 0.0056	−0.01
Post. Corona Radiata	−0.001	−0.0051, 0.003	−0.02	−0.003	−0.018, 0.012	−0.07	5.40e-05	−0.0086, 0.0087	0.00
Ant. Limb Int. Capsule	−0.0041*	−0.0077, −0.00054	−0.09	−0.0018	−0.015, 0.012	−0.04	0.0025	−0.0052, 0.01	0.06
Post. Limb Int. Capsule	−0.00038	−0.0031, 0.0024	−0.01	0.004	−0.0066, 0.015	0.13	−0.003	−0.009, 0.003	−0.09
	MD								
	Vascular Burden			APOE ε4			Vascular Burden * APOE ε4		
	Beta	95% C.I.	Effect Size¥	Beta	95% C.I.	Effect Size	Beta	95% C.I.	Effect Size

	FA								
	Vascular Burden			APOE ε4			Vascular Burden * APOE ε4		
	Beta	95% C.I.	Effect Size¥	Beta	95% C.I.	Effect Size	Beta	95% C.I.	Effect Size
Sup. Long. Fasc.	3.40e-06*	4.2e-07, 6.3e-06	0.09	−4.10e-07	−1.2e-05, 1.1e-05	−0.01	4.10e-06	−2.3e-06, 1e-05	0.11
Sup. Fronto-Occ. Fasc.	7.00e-06	−4.8e-07, 1.5e-05	0.07	−1.30e-06	−3e-05, 2.7e-05	−0.01	6.50e-06	−9.6e-06, 2.3e-05	0.07
Inf. Fronto-Occ. Fasc.	−1.30e-06	−5.2e-06, 2.5e-06	−0.02	9.60e-06	−5e-06, 2.4e-05	0.17	−1.40e-06	−9.7e-06, 6.8e-06	−0.03
Sagittal stratum	1.90e-06	−1.5e-06, 5.3e-06	0.05	3.10e-06	−9.7e-06, 1.6e-05	0.07	3.70e-06	−3.5e-06, 1.1e-05	0.09
Cingulum (gyrus)	2.90e-06*	8.4e-09, 5.7e-06	0.07	−4.30e-07	−1.1e-05, 1e-05	−0.01	2.40e-06	−3.8e-06, 8.6e-06	0.06
Cingulum (hipp.)	−2.90e-06	−7.5e-06, 1.7e-06	−0.05	−1.80e-05*	−3.6e-05, −8.1e-07	−0.31	9.40e-06	−3.9e-07, 1.9e-05	0.16
Fornix (crus)	1.50e-07	−4.8e-06, 5.1e-06	0.00	−3.70e-06	−2.2e-05, 1.5e-05	−0.05	4.40e-06	−6e-06, 1.5e-05	0.06
Fornix (body)	1.20e-05	−4.8e-06, 2.9e-05	0.05	−4.20e-05	−0.00011, 2.2e-05	−0.16	1.30e-05	−2.3e-05, 4.9e-05	0.05
CC. Genu	1.00e-05	−1.8e-06, 2.2e-05	0.06	−9.50e-06	−5.5e-05, 3.6e-05	−0.06	1.10e-06	−2.5e-05, 2.7e-05	0.01
CC. Body	1.10e-05†	4.5e-06, 1.8e-05	0.12	6.20e-06	−1.9e-05, 3.1e-05	0.07	−3.30e-06	−1.7e-05, 1.1e-05	−0.04
CC. Splenium	3.00e-06	−3.2e-06, 9.3e-06	0.04	−7.00e-07	−2.4e-05, 2.3e-05	−0.01	1.80e-06	−1.1e-05, 1.5e-05	0.02
Ant. Corona Radiata	3.10e-06	−9.5e-07, 7.2e-06	0.05	−3.60e-06	−1.9e-05, 1.2e-05	−0.06	6.10e-06	−2.7e-06, 1.5e-05	0.10
Sup. Corona Radiata	5.30e-06†	1.7e-06, 9e-06	0.11	−2.50e-06	−1.6e-05, 1.1e-05	−0.05	4.00e-06	−3.9e-06, 1.2e-05	0.08
Post. Corona Radiata	3.40e-06	−1.1e-06, 7.9e-06	0.06	4.90e-06	−1.2e-05, 2.2e-05	0.09	8.60e-07	−8.8e-06, 1.1e-05	0.02
Ant. Limb Int. Capsule	5.20e-06	−4.2e-07, 1.1e-05	0.07	3.70e-06	−1.8e-05, 2.5e-05	0.05	−1.60e-06	−1.4e-05, 1e-05	−0.02
Post. Limb Int. Capsule	2.90e-06*	1.2e-07, 5.6e-06	0.08	3.10e-06	−7.3e-06, 1.3e-05	0.09	6.80e-07	−5.2e-06, 6.6e-06	0.02

*significant at $p < 0.05$.

†significant at $p < 0.01$.

¥Effect sizes represents the effect for one-unit change in vascular burden score.

Table 4

The associations between vascular burden and APOE ε4 carrier status on change in DTI parameters. Results are from separate models for each predictor variable, controlling for baseline age, sex, race, and scanner.

	FA						MD					
	Vascular Burden			APOE ε4			Vascular Burden			APOE ε4		
	Beta	95% C.I.	Effect Size¥	Beta	95% C.I.	Effect Size	Beta	95% C.I.	Effect Size¥	Beta	95% C.I.	Effect Size
Superior Longitudinal. Fasdculus	−0.00012	−0.00058, 0.00034	−0.02	−0.00044	−0.0014, 0.00054	−0.06	9.10e-08	−3.7e-07, 5.6e-07	0.01	1.20e-07	−9e-07, 1.1e-06	0.02
Sup. Fronto-Occ. Fasc.	−0.00031	−0.0011, 0.00047	−0.03	−0.00087	−0.0025, 0.00079	−0.08	−2.10e-07	−1.7e-06, 13e-06	−0.01	−4.90e-07	−3.7e-06, 2.7e-06	−0.02
Inf Fronto-Occ. Fasc.	1.90e-05	−0.00049, 0.00053	0.00	0.00019	−0.00087, 0.0012	0.02	−2.90e-07	−1.2e-06, 6.1e-07	−0.02	−1.10e-06	−3e-06, 7.7e-07	−0.08
Sagittal stratum	2.20e-05	−0.00064, 0.00068	0.00	−0.00025	−0.0016, 0.0011	−0.02	−1.80e-07	−1.1e-06, 72e-07	−0.01	−2.60e-07	−2.3e-06, 1.8e-06	−0.02
Cingulum (gyrus)	−4.50e-0.5	−0.00055, 0.00046	−0.01	−0.00054	−0.0016, 0.00054	−0.08	−3.10e-07	−8.6e-07, 2Ae-07	−0.04	−2.30e-07	−1.4e-06, 9.4e-07	−0.03
Cingulum (hipp.)	−0.00181†	−0.003, −0.00062	−0.09	0.00067	−0.0018, 0.0031	0.03	130e-06	−1.2e-07, 2.7e-06	0.06	−1.20e-06	−4.1e-06, 1.8e-06	−0.05
Fornix (crus)	−0.00062*	−0.0012, −4.3e-05	−0.07	0.00056	−0.00065, 0.0018	0.06	4.40e-07	−9.5e-07, 1.8e-06	0.02	−2.10e-06	−5.le-06, 8.4e-07	−0.09
Fornix (body)	−6.70e-05	−0.00072, 0.00059	−0.01	0.0014	−6.8e-06, −0.0028	0.16	−2.00e-06	−5e-06, 1.1e-06	−0.05	−2.30e-06	−8.8c-06, 4.2e-06	−0.05
CC. Genu	0.00029	−0.00068, 0.0013	0.02	−0.0027*	−0.0047, −0.00064	−0.18	−6.60e-07	−3.5e-06, 2.2e-06	−0.01	1.40e-06	−4.7e-06, 7.5e-06	0.03
CC. Body	−6.00e-04	−0.0014, 0.00019	−0.05	−0.00082	−0.0025, 0.00087	−0.07	1.90e-06	−3.7e-08, 3.8e-06	0.06	1.30e-06	−2.7e-06, 5.3e-06	0.04
CC. Splenium	−0.00062*	−0.0012, −1.5e-05	−0.06	−0.0015*	−0.0027, −0.00021	−0.15	250e-06†	9.5e-07, 4e-06	0.10	1.70e-06	−1.5e-06, 4.9e-06	0.07
Ant. Corona Radiata	6.70e-05	−0.00037, 5e-04	0.01	−7.00e-04	−0.0016, 0.00023	−0.12	4.60e-08	−6.4e-07, 73e-07	0.00	9.70e-07	−4.9e-07, 2.4e-06	0.09
Sup. Corona Radiata	0.00016	−0.00019, 0.00051	0.03	−3.00e-05	−0.00077, 0.00071	−0.01	−2.90e-08	−6.1e-07, 5be-07	0.00	−5.20e-08	−1.3e-06, 1.2e-06	−0.01
Post. Corona Radiata	−3.30c-05	−0.00057, 5e-04	0.00	−3.00e-0.5	−0.0012, 0.0011	0.00	4.60e-07	−2.1e-07, 1.1e-06	0.05	−2.80e-07	−1.7e-06, 1.2e-06	−0.03
Ant. Limb Inc Capsule	3.10e-05	−0.00081, 0.00088	0.00	−0.00057	−0.0024, 0.0012	−0.04	5.70e-08	−1.3e-06, 1.4e-06	0.00	7.40e-07	−2.1e-06, 3.6e-06	0.03
Post. Limb Inc Capsule	−0.00014	−0.00065, 0.00037	−0.02	−0.00064	−0.0017, 0.00043	−0.08	−3.70e-07	−9.6e-07, 23e-07	−0.04	−8.00e-07	−2.1e-06, 4.8e-07	−0.09

*significant at $p < 0.05$.

†Significant at $p < 0.01$.

¥Effect sizes represents the effect for one-unit change in vascular burden score.

Table 5

The associations between vascular burden, APOE ε4 carrier status, and their interaction term, on the rates of change in DTI parameters. Results are from the same model controlling for baseline age, sex, race, and scanner.

	FA								
	Vascular Burden*Time			APOE status*Time			Vascular Burden*APOE status*Time		
	Beta	95% C.I.	Effect Size¥	Beta	95% C.I.	Effect Size	Beta	95% C.I.	Effect Size
Sup. Long. Fasc.	8.20e-06	−0.00051, 0.00053	0.00	0.00012	−0.0021, 0.0024	0.02	−0.00049	−0.0016, 0.00065	−0.07
Sup. Fronto-Occ. Fasc.	−3.00e-04	−0.0012, 0.00059	−0.03	−7.00e-04	−0.0045, 0.0031	−0.06	5.70E-05	−0.0019, 0.002	0.01
Inf. Fronto-Occ. Fasc.	3.00e-05	−0.00061, 0.00055	0.00	0.00019	−0.0026, 0.0023	−0.02	0.00021	−0.001, 0.0015	0.03
Sagittal stratum	0.00018	−0.00056, 0.00092	0.02	0.001	−0.0022, 0.0043	0.10	−0.00068	−0.0023, 0.00094	−0.06
Cingulum (gyrus)	−9.90e-06	−0.00058, 0.00056	0.00	−0.00033	−0.0028, 0.0022	−0.05	−8.70e-05	−0.0014, 0.0012	−0.01
Cingulum (hipp.)	−0.0015*	−0.0028, −0.00019	−0.07	0.0041	−0.0015, 0.0098	0.20	0.0016	−0.0044, 0.0013	−0.08
Fornix (crus)	−0.00083*	−0.0015, −0.00018	−0.09	−0.00083	−0.0036, 0.002	−0.09	0.00088	−0.00053, 0.0023	0.10
Fornix (body)	−0.00035	−0.0011, 0.00039	−0.04	−0.00081	−0.004, 0.0024	−0.09	0.0012	−0.00045, 0.0027	0.13
CC. Genu	0.00012	−0.00097, 0.0012	0.01	−0.0048*	−0.0095, 8.4e-05	−0.33	0.0011	−0.0013, 0.0035	0.08
CC. Body	−0.00061	−0.0015, 0.00028	−0.05	−0.0017	−0.0056, 0.0021	−0.14	0.00018	−0.0018, 0.0021	0.02
CC. Splenium	−0.00053	−0.0012, 0.00015	−0.05	−0.0014	−0.0043, 0.0015	−0.14	−0.00015	−0.0016, 0.0013	−0.01
Ant. Corona Radiata	5.40e-05	−0.00044, 0.00055	0.01	−0.0013	−0.0034, 0.00087	−0.22	2.00e-04	−0.00089, 0.0013	0.03
Sup. Corona Radiata	0.00035	−4.4e-05, 0.00075	0.07	0.0013	−0.00037, 0.003	0.28	−0.00087*	−0.0017, 1.1e-05	−0.19
Post. Corona Radiata	0.00018	−0.00042, 0.00079	0.03	0.0016	−0.00098, 0.0042	0.23	−0.001	−0.0023, 0.00031	−0.14
Ant. Limb Int. Capsule	0.00038	−0.00057, 0.0013	0.03	0.0022	−0.0019, 0.0063	0.17	−0.0016	−0.0036, 0.00048	−0.12
Post. Limb Int. Capsule	−7.20e-05	−0.00065, 0.00051	−0.01	−0.00037	−0.0028, 0.0021	−0.05	−0.00019	−0.0014, 0.0011	−0.02
	MD								
	Vascular Burden*Time			APOE status*Time			Vascular Burden*APOE status*Time		
	Beta	95% C.I.	Effect Size¥	Beta	95% C.I.	Effect Size	Beta	95% C.I.	Effect Size
Sup. Long. Fasc.	2.10e-07	−3.1e-07, 7.2e-07	0.03	1.70e-06	−5.7e-07, 4.1e-06	0.24	−7.00e-07	−1.9e-06, 4.9e-07	−0.10
Sup. Fronto-Occ. Fasc.	−6.60e-07	−2.3e-06, 1e-06	−0.03	−4.90e-06	−1.2e-05, 2.5e-06	−0.25	2.40e-06	−1.4e-06, 6.3e-06	0.12

	FA								
	Vascular Burden*Time			APOE status*Time			Vascular Burden*APOE status*Time		
	Beta	95% C.I.	Effect Size¥	Beta	95% C.I.	Effect Size	Beta	95% C.I.	Effect Size
Inf. Fronto-Occ. Fasc.	−4.90e-08	−1.1e-06, 9.8e-07	0.00	6.10e-07	−3.7e-06, 4.9e-06	0.04	−9.90e-07	−3.2e-06, 1.2e-06	−0.07
Sagittal stratum	−2.30e-07	−1.3e-06, 8.5e-07	−0.02	−7.60e-07	−5.5e-06, 4e-06	0.05	1.80e-07	−2.2e-06, 2.6e-06	0.01
Cingulum (gyrus)	−2.10e-07	−8.3e-07, 4.1e-07	−0.03	6.80e-07	−2e-06, 3.4e-06	−0.09	−4.70e-07	−1.8e-06, 8.9e-07	−0.06
Cingulum (hipp.)	1.90e-06*	3.3e-07, 3.5e-06	0.08	3.20e-06	−3.6e-06, 1e-05	0.14	−2.60e-06	−6e-06, 8.3e-07	−0.12
Fornix (crus)	1.00e-06	−5.5e-07, 2.6e-06	0.04	2.00e-06	−4.8e-06, 8.7e-06	0.09	−2.40e-06	−5.8e-06, 1e-06	−0.11
Fornix (body)	2.70e-07	−3.2e-06, 3.7e-06	0.01	1.50e-05*	4.1e-07, 3e-05	0.35	1.00e-05†	−1.8e-05, −2.7e-06	−0.24
CC. Genu	3.40e-07	−2.9e-06, 3.6e-06	0.01	9.40e-06	−4.5e-06, 2.3e-05	0.21	4.80e-06	−1.2e-05, 2.3e-06	−0.11
CC. Body	2.20e-06*	7.4e-08, 4.4e-06	0.07	4.30e-06	−4.9e-06, 1.4e-05	0.13	1.90e-06	−6.5e-06, 2.8e-06	−0.06
CC. Splenium	3.00e-06y	1.3e-06, 4.7e-06	0.12	6.40e-06	−1e-06, 1.4e-05	0.25	2.90e-06	−6.6e-06, 8.2e-07	−0.11
Ant. Corona Radiata	1.00e-07	−6.6e-07, 8.6e-07	0.01	1.50e-06	−1.8e-06, 4.9e-06	0.13	4.10e-07	−2.1e-06, 1.3e-06	−0.04
Sup. Corona Radiata	−6.40e-09	−6.6e-07, 6.4e-07	0.00	5.50e-07	−2.3e-06, 3.4e-06	0.07	1.50e-07	−1.7e-06, 1.4e-06	−0.02
Post. Corona Radiata	4.40e-07	−3.2e-07, 1.2e-06	0.04	−1.00e-07	−3.4e-06, 3.2e-06	−0.01	1.10e-07	−1.6e-06, 1.8e-06	0.01
Ant. Limb Int. Capsule	−2.10e-07	−1.7e-06, 1.3e-06	−0.01	−1.00e-06	−7.5e-06, 5.5e-06	−0.05	1.10e-06	−2.1e-06, 4.4e-06	0.05
Post. Limb Int. Capsule	−2.90e-07	−9.5e-07, 3.8e-07	−0.03	4.10e-07	−2.5e-06, 3.3e-06	0.04	3.90e-07	−1.9e-06, 1.1e-06	−0.04

*significant at $p < 0.05$.

†significant at $p < 0.01$.

¥Effect sizes represents the effect for one-unit change in vascular burden score.